nature medicine

LETTERS

https://doi.org/10.1038/s41591-018-0204-6

High prevalence of *Streptococcus pyogenes* Cas9-reactive T cells within the adult human population

Dimitrios L. Wagner[1,2,3], Leila Amini[1,2], Desiree J. Wendering[1,2], Lisa-Marie Burkhardt[1], Levent Akyüz[1], Petra Reinke[2,4], Hans-Dieter Volk[1,2,4,5] and Michael Schmueck-Henneresse[1,2,4,5*]

The discovery of the highly efficient site-specific nuclease system CRISPR–Cas9 from *Streptococcus pyogenes* has galvanized the field of gene therapy[1,2]. The immunogenicity of Cas9 nuclease has been demonstrated in mice[3,4]. Preexisting immunity against therapeutic gene vectors or their cargo can decrease the efficacy of a potentially curative treatment and may pose significant safety issues[3–6]. *S. pyogenes* is a common cause for infectious diseases in humans, but it remains unclear whether it induces a T cell memory against the Cas9 nuclease[7,8]. Here, we show the presence of a preexisting ubiquitous effector T cell response directed toward the most widely used Cas9 homolog from *S. pyogenes* (SpCas9) within healthy humans. We characterize SpCas9-reactive T cells within the CD4/CD8 compartments for multi-effector potency, cytotoxicity, and lineage determination. In-depth analysis of SpCas9-reactive T cells reveals a high frequency of SpCas9-reactive regulatory T cells that can mitigate SpCas9-reactive effector T cell proliferation and function in vitro. Our results shed light on T cell–mediated immunity toward CRISPR-associated nucleases and offer a possible solution to overcome the problem of preexisting immunity.

S. pyogenes Cas9 (SpCas9) was the first CRISPR-associated nuclease (Cas) used to introduce double-strand breaks at specific DNA sequences[1]. Through ease of target adaption and remarkable efficacy, it became the most widely adopted tool for rewriting genes in research and potential clinical applications[2]. High-fidelity Cas9 enzymes and Cas9-directed base editors were developed to reduce the risk of off-target activity and chromosomal aberrations[9,10,11]. Most variants are based on the SpCas9 enzyme originating from the facultative pathogenic bacterium *S. pyogenes*. Approximately 12% of children under 18 have an asymptomatic colonization of the faucial mucosa with *S. pyogenes*[12]. *S. pyogenes*-associated pharyngitis and pyoderma are among the most common diseases related to *S. pyogenes* infection worldwide[7]. Considering the high prevalence of *S. pyogenes* infection, we hypothesized that SpCas9 could elicit an adaptive memory immune response in humans. Most therapeutic applications aim to temporarily express Cas9 nuclease or deliver the protein directly into the target cells. Thus, SpCas9-specific antibodies may be negligible[4,8]. However, intracellular protein degradation processes lead to peptide presentation of Cas9 fragments on the cellular surface of gene-edited cells that may be recognized by SpCas9-reactive T cells.

To detect a putative SpCas9-directed T cell response, we stimulated human peripheral blood mononuclear cells (PBMCs) with recombinant SpCas9 and analyzed the reactivity of $CD3^+$, $CD4^+$, and $CD8^+$ T cells by flow cytometry with a set of markers for T cell activation (CD137, CD154) and effector cytokine production (interferon-γ (IFN-γ), tumor necrosis factor-α (TNF-α), interleukin 2 (IL-2)) (Fig. 1a–d and Supplementary Fig. 1a,b)[13,14]. We relied on protein uptake, processing, and presentation of SpCas9 peptides by professional antigen-presenting cells (APCs) to both major histocompatibility complex class I (MHC class I; cross-presentation) and MHC class II within the PBMCs. Intriguingly, 96% of the donors evaluated (46/48) showed an effector T (T_{eff}) cell activation upon SpCas9 stimulation, indicated by CD137 upregulation in both CD4 and CD8 T cell compartments (Fig. 1a–c). After background normalization, 96% of the responding donors presented an average of 0.24% (range: 0.03–1.3%) $CD137^+$ T cells within the $CD4^+$ and $CD8^+$ subsets (Fig. 1b,c,e). We detected SpCas9-reactive multipotent T_{eff} cells expressing at least one or even several effector cytokines ($CD4^+ > CD8^+$ T cells) (Fig. 1f,g). We analyzed CD107a expression in a subset of donors (12/48) and found upregulation in 50% of them (6/12) (Supplementary Fig. 1c,d). Previous exposure to *S. pyogenes* in our cohort was verified by assessing antibody titers against two *S. pyogenes* antigens. In accordance with our high rate of SpCas9-induced T cell activation, we detected antibody titers against at least one of two exemplary *S. pyogenes* antigens in 85% of our donors (Supplementary Table 1). Most SpCas9-reactive T cells expressed an effector-memory (T_{em}) ($CD4^+$ and $CD8^+$) or terminally differentiated effector memory T (T_{emra}) cell ($CD8^+$) phenotype implying repetitive previous exposure to SpCas9 and was comparable with the memory T cell response to cytomegalovirus (CMV) (Supplementary Fig. 1e–i)[15]. In contrast, we could not detect unspecific T cell activation in PBMCs derived from cord blood through SpCas9 treatment because these T cells are antigen-inexperienced and exclusively express a naive T cell phenotype (Supplementary Fig. 2). Hence, we concluded that SpCas9 stimulation induces a T_{em} response in adult humans.

Recent studies indicate that continuous colonization and repetitive exposure to environmental proteins or pathogens at the mucosal surfaces induce regulatory T (T_{reg}) cells[16,17]. These T_{reg} cells balance immune responses and may even regulate tolerance against innocuous environmental antigens[17]. This expanded the significance of T_{reg} from controlling autoreactivity toward a general role in protecting against tissue-damaging inflammation. To determine the contribution of T_{reg} cells to the SpCas9-induced T cell response, we performed CD25 surface staining and intracellular staining of the transcription factor FOXP3 [18,19]. Further, we combined T_{reg}-defining markers

[1]Institute for Medical Immunology, Charité – Universitätsmedizin Berlin, Berlin, Germany. [2]Berlin-Brandenburg Center for Regenerative Therapies (BCRT), Charité – Universitätsmedizin Berlin, Berlin, Germany. [3]Berlin Institute of Health (BIH), Berlin, Germany. [4]Berlin Center for Advanced Therapies (BeCAT), Charité – Universitätsmedizin Berlin, Berlin, Germany. [5]These authors jointly directed this study: Hans-Dieter Volk, Michael Schmueck-Henneresse. *e-mail: michael.schmueck-henneresse@charite.de

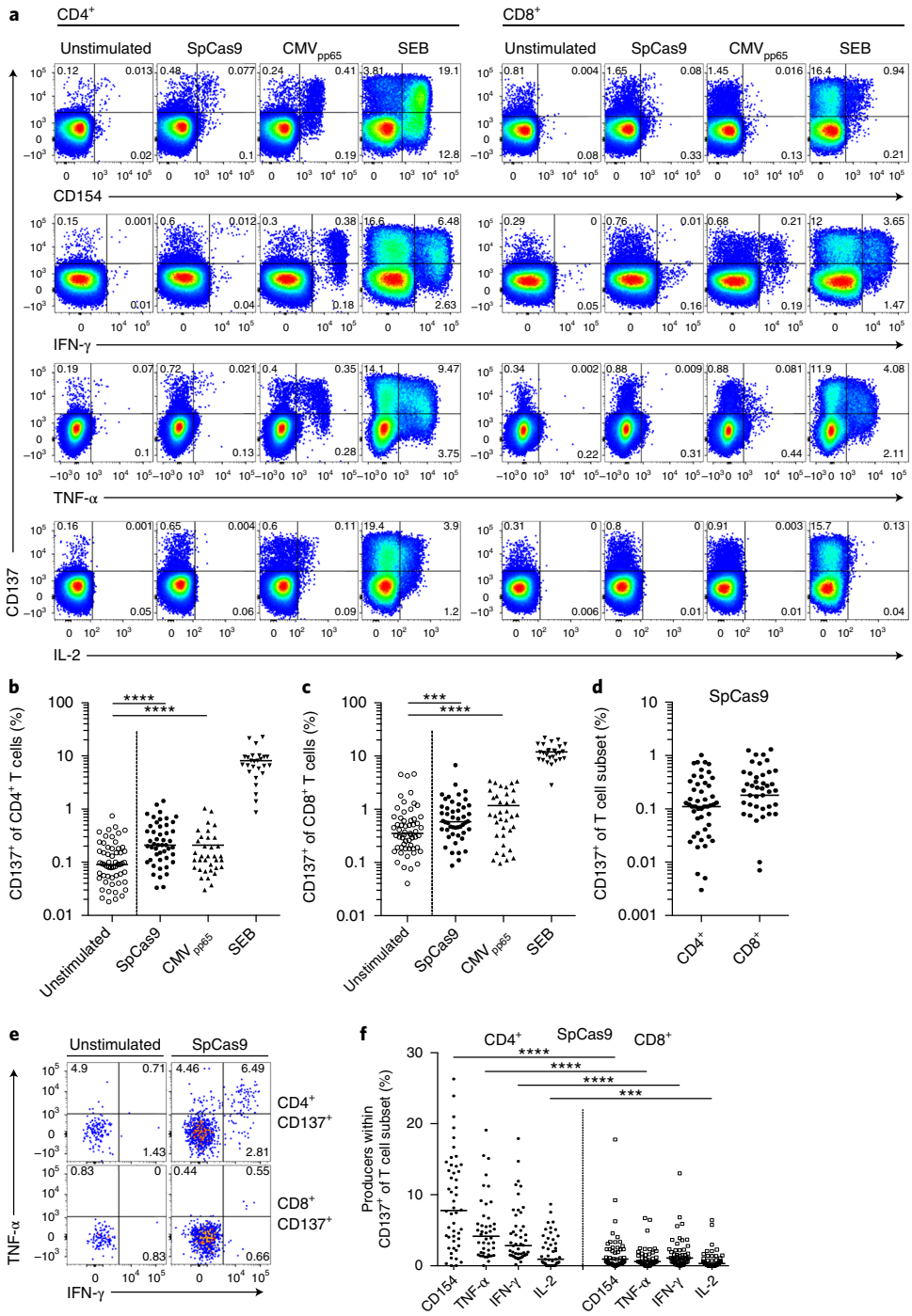

Fig. 1 | Ubiquitous peripheral SpCas9-reactive T cell response in human donors. Short-term ex vivo stimulation with SpCas9 whole protein induces polyfunctional effector CD4+ and CD8+ T cell responses. PBMCs were stimulated with SpCas9 whole protein for 16 h. The frequencies of T cell responses were assessed by flow cytometry. The experimental design for ex vivo detection of SpCas9-reactive T cell responses is shown in Supplementary Fig. 1. Lymphocytes were gated on the basis of the forward side scatter (FSC) versus side scatter (SSC) profile and subsequently gated on FSC-Height versus FSC to exclude doublets. **a**, Representative FACS images show SpCas9-induced activation defined by CD137 expression plotted against CD154, IFN-γ, TNF-α, and IL-2 for CD4+ (left) and CD8+ (right) T cells compared to unstimulated , CMV_{pp65}-stimulated, and SEB-stimulated PBMCs . **b**,**c**, SpCas9, CMV-pp65 or SEB-induced activation (CD4+ (**b**); CD8+ (**c**)), defined by CD137 expression, compared to unstimulated controls (unstimulated $n = 48$ healthy donors; SpCas9 $n = 48$ healthy donors; CMV-pp65 $n = 35$ healthy donors; SEB $n = 26$ healthy donors). Data are quantified according to gating strategy in **a** and Supplementary Fig. 1. Median values are shown; statistical analysis by Wilcoxon signed-rank test. $^{***}P < 0.001$, $^{****}P < 0.0001$. For selected healthy donors, we repeated the experiment three times with similar results. **d**, Background-normalized CD137 expression in response to SpCas9 whole protein by CD4+ and CD8+ T cells (ΔCD4+CD137+ > 0, indicating a measurable T cell response higher than background activation, in 46/48 donors; ΔCD8+CD137+ > 0 in 38/48 donors). **e**, Representative FACS plots of IFN-γ and TNF-α production within SpCas9-activated CD4+ CD137+ and CD8+ CD137+ T cells ($n = 48$ healthy donors). **f**, SpCas9-induced expression of CD154, TNF-α, IFN-γ, and IL-2 within activated CD4+CD137+ and CD8+CD137+ T cells ($n = 48$ healthy donors). Median values are shown; statistical analysis by Wilcoxon signed-rank test. $^{***}P = 0.0001$ (IL-2); $^{****}P < 0.0001$ (CD154, TNF-α, IFN-γ). The experiments were performed with a dedicated number of healthy individuals (n) as biologically independent samples/independent experiments.

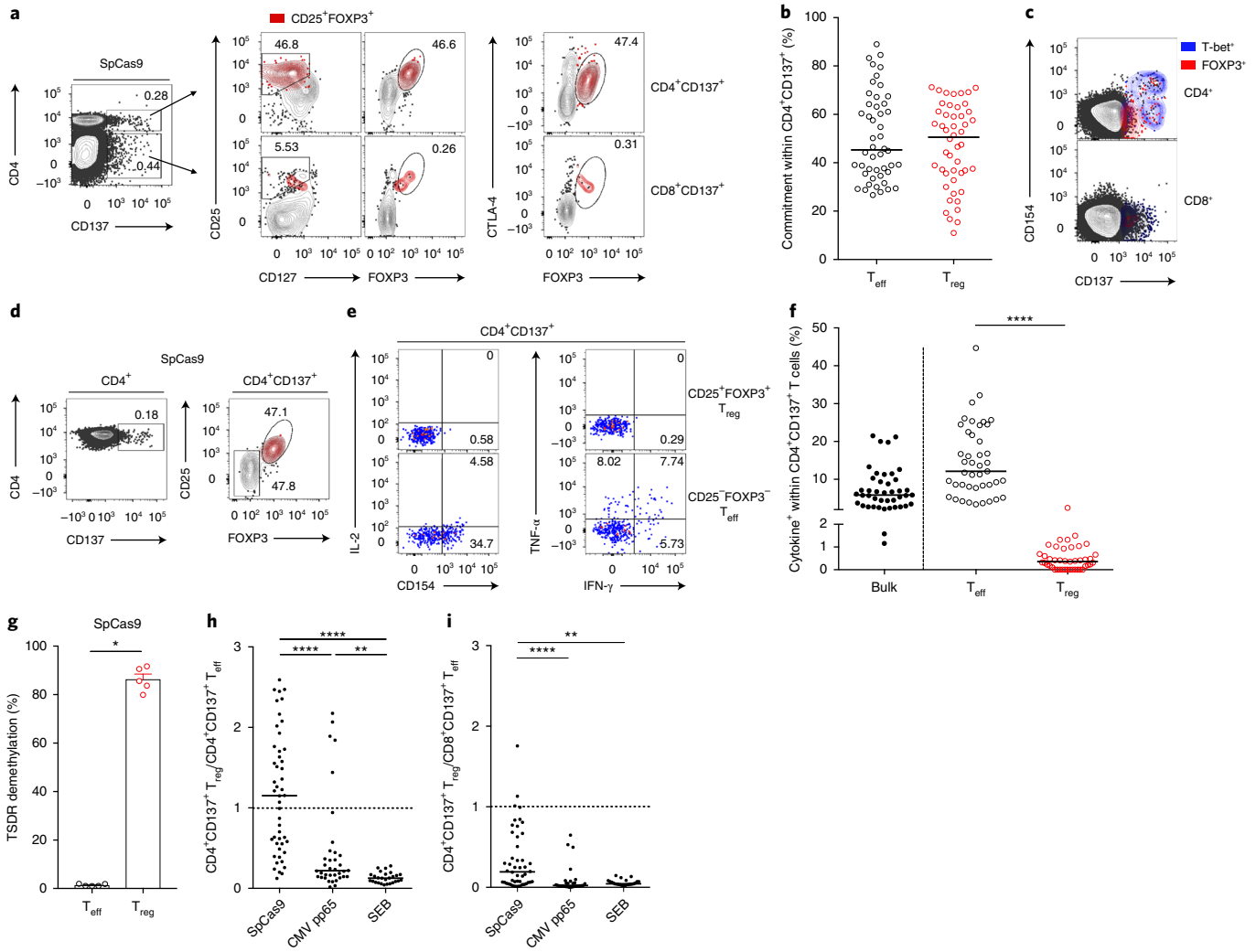

Fig. 2 | SpCas9-reactive T cell response contains a substantial proportion of T_{reg} cells. Identification of T_{eff} and T_{reg} phenotypes within CD137$^+$ T cells after 16-h stimulation of human PBMCs with SpCas9 whole protein. **a**, Representative FACS plots show expression of the T_{reg}-defining markers CD25, FOXP3, CTLA-4, and CD127 within SpCas9-activated CD4$^+$CD137$^+$ and CD4$^-$CD137$^+$ T cells. The overlay highlighted in red represents the CD25$^+$FOXP3$^+$ of CD137$^+$ T cells. $n=6$ healthy donors. **b**, Relative contribution of the T_{eff} and CD25$^+$FOXP3$^+$ T_{reg} phenotypes to the SpCas9-induced CD4$^+$CD137$^+$ T cell response. Median values are shown. The experiment was performed in 48 healthy donors as biologically independent samples/independent experiments. **c**, Overlay contour plots of a representative donor demonstrate T-bet$^+$ (blue) and FOXP3$^+$ (red) T cells within SpCas9-induced T cell activation as defined by CD137 and CD154 expression. $n=6$ healthy donors. This experiment was repeated twice with similar results. **d**, Gating of CD4$^+$ T_{reg} within SpCas9-induced CD4$^+$CD137$^+$ T cells. **e**, Corresponding CD154 expression and cytokine production within CD4$^+$CD137$^+$ T_{reg} and T_{eff} (red and black, respectively, in **d**) cells. **f**, Summary of accumulated cytokine production (IFN-γ, TNF-α, IL-2) within bulk CD4$^+$CD137$^+$ T cells, CD4$^+$CD137$^+$ T_{eff} (CD25$^-$FOXP3$^-$) cells, and CD4$^+$CD137$^+$ T_{reg} (CD25$^+$FOXP3$^+$) cells. $n=43$ healthy donors. Median values are shown; statistical analysis by Wilcoxon signed-rank test; $^{****}P<0.0001$. **g**, DNA methylation analysis of the TSDR in SpCas9-reactive ex vivo isolated CD137$^+$CD154$^{+/-}$CD25$^-$CD127$^+$FOXP3$^-$ (T_{eff}) and CD137$^+$CD154$^-$CD25$^+$CD127$^-$FOXP3$^+$ (T_{reg}) cells (average TSDR demethylation: T_{reg} 86.3%; T_{eff} 1.39%; $n=5$ healthy donors). For SpCas9-reactive T_{eff} and T_{reg} isolation, PBMCs were cultured in the presence of 5 μg ml^{-1} SpCas9 whole protein and 1 μg ml^{-1} CD40-specific antibody for 16 h. SpCas9-reactive T_{reg}/T_{eff} cells were enriched by FACS according to Supplementary Fig. 5. Mean values are shown. Statistical analysis by two-tailed paired *t*-test. $^*P<0.05$. **h**, Balanced T_{eff}/T_{reg} cell response to SpCas9 whole protein. Relationship of antigen-reactive T_{reg} to CD4$^+$ T_{eff} cells is shown for SpCas9 whole protein, CMV_{pp65} peptides, and SEB stimulation. Antigen-reactive T_{reg} and T_{eff} cells were defined according to the gating strategy presented in **d**. Ratio of T_{reg} frequency versus the proportion of T_{eff} cells within CD4$^+$CD137$^+$ antigen-reactive cells. **i**, Ratio of antigen-reactive T_{reg} versus CD8$^+$ T_{eff} cells shown for SpCas9 whole protein, CMV_{pp65} peptides, and SEB stimulation (SpCas9: $n=48$ healthy donors; CMV pp65: $n=35$ healthy donors; SEB: $n=26$ healthy donors). The median is shown. Statistical analysis by Kruskal–Wallis test and Dunn's multiple comparisons test. $^{**}P<0.01$, $^{****}P<0.0001$.

with activation markers and cytokine profiling following SpCas9 stimulation (Fig. 2a,d and Supplementary Fig. 3a). Intriguingly, we found elevated frequencies of T_{reg} cells within SpCas9-reactive CD4$^+$CD137$^+$ T cells, which comprised between 11 and 71.2% of the total CD4$^+$ response (Fig. 2a,b). We confirmed T_{reg} cell identity by using additional phenotypic marker combinations, such as FOXP3$^+$CTLA-4$^+$ or CD127^{lo}CD25^{hi} (Fig. 2a and Supplementary Fig. 3a,b)[20]. Further investigation of SpCas9-induced T cell activation revealed distinct transcription factor profiles (CD4$^+$FOXP3$^+$ T_{reg}:CD137^{dim}CD154$^-$; CD4$^+$T-bet$^+$$T_{eff}$:CD137$^+$CD154$^+$ and CD137^{hi}) (Fig. 2c and Supplementary Fig. 3)[21]. Functionally, T_{reg} cells did not contribute to SpCas9-induced cytokine production (Fig. 2d–f and Supplementary Fig. 3c–g); however, they displayed a memory phenotype (Supplementary Fig. 4a,b). Moreover, we

enriched SpCas9-reactive T_{eff} and T_{reg} cells using fluorescence-activated cell sorting (FACS) (Supplementary Fig. 5), which allowed epigenetic analysis of the T_{reg}-specific demethylation region (TSDR)[22]. In contrast to SpCas9-activated T_{eff} cells, SpCas9-reactive T_{reg} cells displayed high TSDR demethylation (Fig. 2g). The proportion of T_{reg} cells within activated T cells following stimulation with CMV phosphoprotein 65 (CMV_{pp65}) peptides and *Staphylococcus* enterotoxin B (SEB) was consistently lower than under SpCas9-stimulated conditions in all donors measured (Fig. 2h,i).

Analysis of the *T cell receptor β locus* (*TRB*) repertoire in SpCas9-reactive T cell subsets revealed a low diversity and some intraindividual clonal overlap between T_{eff} and T_{reg} cells (Supplementary Fig. 6a–d). The top 100 clones cover more than 36% and 61% of the *TRB* repertoire of SpCas9-activated T_{eff} and T_{reg} cells, respectively. In contrast, the top 100 clones of polyclonal T_{eff} and T_{reg} cells cover only 4% and 8% of the *TRB* repertoire, indicating that SpCas9 treatment leads to an activation of clonally enriched T_{eff} and T_{reg} cell populations. However, the most prevalent clones were distinctly distributed within the different T cell subsets, indicating that the majority of SpCas9-reactive T_{eff} and T_{reg} cells are derived neither from the same precursor cell nor from rare cell clones. We assume that there is a strong clonal bias in vivo with distinct T cell receptor (TCR) specificities, although we cannot exclude that SpCas9-reactive T_{reg} cells are thymus-derived with TCR reactivity to self-antigens. SpCas9-reactive T_{reg} cells possess phenotypic, functional, and epigenetic features of both thymus-derived and peripherally induced T_{reg} cells. Both the T_{reg}/T_{eff} ratio as well as the *TRB* repertoire data are in accordance with previous reports on T_{reg} specificity toward innocuous antigens or fungi[17,23].

Although approximately 10% of all bacteria have class 2 CRISPR–Cas systems, only few have been adapted for gene editing[4,24]. Strikingly, stimulation with the Cas orthologs *Acidaminococcus* sp. Cas12a (also known as Cpf1) and *Staphylococcus aureus* Cas9 (SaCas9) yielded similar frequencies of activated T_{eff} and T_{reg} within the respective antigen response (Supplementary Figs. 4c,d and 7). We compared the protein sequence of SpCas9 with its homologs SaCas9 and Cpf1 and found a shared protein sequence identity of 26% and 38%, respectively. Sequence homology between Cas proteins could lead to activation of T cells with specificity toward Cas epitopes that are shared between different bacterial species. Furthermore, *S. aureus* and *Acidaminococcus* sp. are common facultative pathogenic species; a separate immunization to their bacterial antigens may explain the observed T cell response. In particular, *Acidaminococcus* sp. may induce T_{reg} cells as a critical regulator for immune tolerance in the gastrointestinal tract like other intestinal bacteria[16,25].

We excluded endotoxin contamination in preclinical state recombinant Cas proteins that might induce TNF-α via toll-like receptor signaling on immune cells and could lead to unspecific T_{reg} activation (Supplementary Fig. 8)[26,27]. The SpCas9-induced T cell response in the presence of bactericidal/permeability-increasing protein (BPI) revealed no relevant differences in the frequencies of T_{eff} or T_{reg} cells compared to control stimulation without BPI (Supplementary Fig. 8b–d). Compared to SpCas9-stimulated PBMCs, stimulation of bulk pre-enriched T_{reg} cells revealed no differences in SpCas9-reactive T_{reg} frequencies, excluding unspecific activation of bystander T_{reg} cells through SpCas9-reactive T_{eff} cells[27] (Supplementary Fig. 8e–h). Furthermore, blocking human leukocyte antigen-DR (HLA-DR; anti–MHC class II antibody) resulted in reduced SpCas9-induced $CD4^+$ T cell response (Fig. 3a,b and Supplementary Fig. 9d,e), demonstrating MHC-restricted SpCas9 peptide presentation and recognition by $CD4^+$ T cells. Taken together, our findings indicate that SpCas9-reactive T_{reg} cells are an inherent part of the physiological SpCas9-induced T cell response in the peripheral blood of adult humans.

Consequently, we investigated the capacity of SpCas9-reactive T_{reg} cells to suppress their T_{eff} counterparts. When all $CD25^+$ T_{reg} cells were depleted from PBMCs, we observed significantly increased cytokine production within $CD4^+CD137^+CD154^+$ T_{eff} cells after SpCas9 treatment, but not within the CMV pp65- or SEB-stimulated response (Fig. 3a,c). Neither depletion of CD25 nor depletion of CD4 from PBMCs significantly altered the SpCas9-reactive $CD8^+$ T cell response, indicating that the $CD8^+$ T_{eff} response is not the result of bystander reactivity (Supplementary Fig. 9a–c).

Fig. 3 | SpCas9-reactive T_{reg} cells suppress their SpCas9-reactive T_{eff} counterpart. a, Representative FACS plots of IFN-γ production versus $FOXP3^+$ expression within SpCas9-activated $CD4^+CD137^+$ and $CD4^+CD137^+CD154^+$ T cells in the presence or absence of 15 μg ml^{-1} HLA-DR-blocking antibody (anti–MHC class II) or following $CD25^+$ depletion after 16-h stimulation of human PBMCs with SpCas9 whole protein, CMV_{pp65}, or SEB. $n = 12$ healthy donors. **b**, Antigen-reactive $CD4^+$ T cell proportion and function in the presence of anti–MHC class II α chain antibodies. The dotted line indicates normalized antigen-induced $CD4^+$ T cell response without anti–MHC class II antibodies. The percentages of residual $CD4^+$ T cells expressing the indicated markers are shown. **c**, Antigen-reactive $CD4^+$ T cell proportion and function following CD25 depletion from PBMCs. The dotted line indicates the normalized antigen-induced $CD4^+$ T cell response without depletion of CD25-expressing cells. The percentage of residual $CD4^+$ T cells expressing the indicated markers are shown. The percentage of residual $CD4^+CD25^+FOXP3^+$ T_{reg} serves as a control and indicates successful depletion within the treated conditions. The experiment was performed in $n = 12$ healthy donors as biologically independent samples/independent experiments. Mean ± s.e.m. is shown; the D'Agostino and Pearson normality test was performed. Wilcoxon signed-rank test or two-tailed paired *t*-test were performed depending on whether data were normally distributed or not. $^*P \leq 0.05$. **d**, SpCas9-reactive $CD4^+$ T_{reg} cells suppress their SpCas9-reactive T_{eff} counterparts dose-dependently. SpCas9-reactive T_{reg} and T_{eff} and polyclonal T_{eff} cells were enriched (Supplementary Fig. 5). T_{eff} proliferation (blue) for SpCas9-reactive (left) and polyclonal (right) T_{eff} cells is shown by CFSE dilution following 96-h culture in the presence or absence of SpCas9-reactive T_{reg} (red) cells at ratios of 1:1 and 1:5. SpCas9-reactive T cells were activated only once before FACS. Polyclonal T_{eff} cells were stimulated with anti-CD3/CD28-coated microbeads. **e**, SpCas9-reactive suppression of SpCas9-reactive T_{eff} counterparts, determined according to the experimental setup of **d**; summary of $n = 6$ healthy donors for $CD4^+$ (left) and $CD8^+$ (right) T cells. **f**, Culture supernatants were collected for cytokine measurements following 96-h culture (MSD multiplex analysis). Cytokine concentrations (IFN-γ; TNF-α; IL-2; and IL-10) in the supernatants of SpCas9-reactive T_{eff} and T_{reg} cultures are shown. $n = 6$ healthy donors. Mean ± s.e.m. is shown. A Kolmogorov–Smirnov test was performed to evaluate Gaussian distribution. Depending on normality testing, either a two-tailed paired *t*-test or Wilcoxon signed-rank test was employed. $^*P \leq 0.05$. **g**, Suppression of cytokine production in the cocultures of SpCas9-reactive T_{reg} and T_{eff} cells. The experiment was performed in $n = 6$ healthy donors. Mean ± s.e.m. is shown. **h**, Assessment of SpCas9-reactive T cell-mediated cytotoxicity by flow cytometric VITAL assay. Specific cytotoxic killing of SpCas9-transfected targets by SpCas9-reactive T_{eff} cells in the presence or absence of SpCas9-reactive T_{reg} cells. Transfected LCLs expressing SpCas9 and GFP (LCLs-$SpCas9^+GFP^+$) served as a SpCas9-positive target, while unmodified *N*,*N*-dimethyldodecylamine *N*-oxide (DDAO)$^+$ LCLs were used as control nontargets. GFP served as a reporter for SpCas9 expression. Cells were cocultured at T cell/target cell ratios of 10:1, 1:1, and 1:10 for 16 h. Samples without T cells, containing only targets and nontargets (LCLs-$SpCas9^+GFP^+$/LCLs), served as the internal control. **i**, Quantification of the SpCas9-reactive T cell–mediated cytotoxicity for $n = 6$ donors according to the experimental setup of **h**. The mean percentage survival of LCLs-$SpCas9^+GFP^+$ target cells was calculated relative to the LCL controls. The experiment was performed in $n = 6$ healthy donors as biologically independent samples/independent experiments. Mean ± s.e.m. is shown.

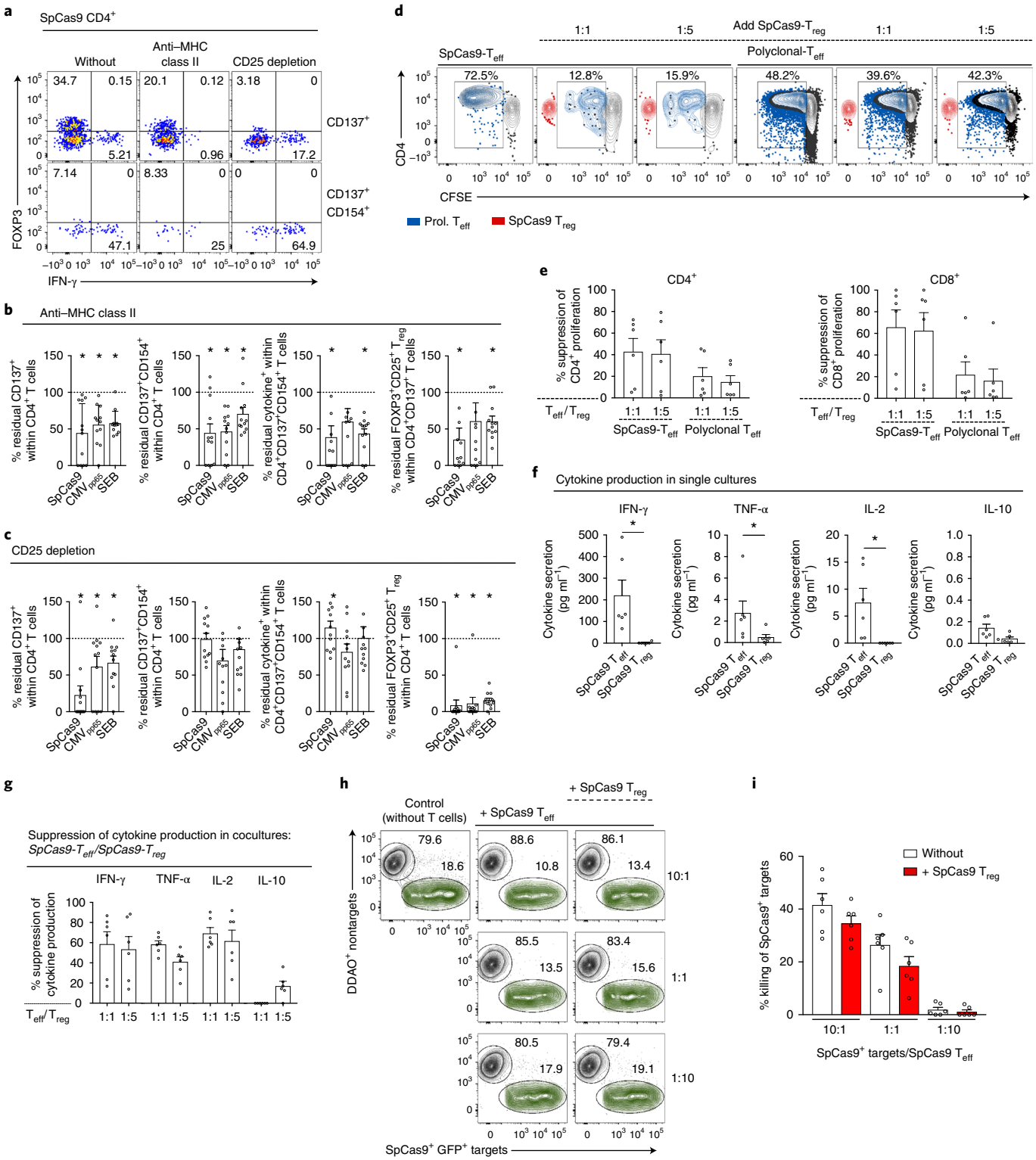

SpCas9-reactive T_{reg} cells could efficiently suppress the proliferation of T_{eff} cells in a SpCas9-dependent manner, with stronger suppression of SpCas9-directed $CD4^+$ T_{eff} and $CD8^+$ T_{eff}, but weaker inhibition of polyclonally activated $CD4^+$ and $CD8^+$ T_{eff} cells (Fig. 3d,e). Enriched SpCas9-reactive T_{reg} cells did not secrete IL-2 and secreted significantly less IFN-γ and TNF-α than their T_{eff} counterparts (Fig. 3f). Moreover, the analysis of the supernatants from the coculture assays revealed a remarkable suppression of proinflammatory cytokine release mediated by SpCas9-activated T_{reg} cells (Fig. 3g). We observed a trend toward an inverse correlation of ex vivo SpCas9-reactive T_{reg}/$CD8^+$ T_{eff} ratio with SpCas9-induced proliferation of $CD8^+$ T_{eff} cells (Supplementary Fig. 9f–h). This could indicate that donors with fewer SpCas9-reactive T_{reg} cells have relatively higher $CD8^+$ T_{eff} responses.

To evaluate the immunity toward endogenously expressed SpCas9, we transfected a SpCas9- and green fluorescent protein (GFP)-containing DNA plasmid into lymphoblastoid B cell lines (LCLs) and challenged them with enriched autologous SpCas9-reactive T_{eff} cells. SpCas9-reactive T_{eff} cells induced specific lysis of SpCas9-expressing LCLs in a dose-dependent manner, but

not GFP-expressing control LCLs (Fig. 3h,i and Supplementary Fig. 10a,b). High expression of a transgene may increase the probability of peptide presentation and thus increase the risk for $CD8^+$ T cell–mediated recognition. This notion is supported by our observation that LCLs with a higher transgene level were targeted preferentially (Supplementary Fig. 10g,h). Thus, CRISPR–Cas9 gene-edited cells will be targeted by the preprimed T_{eff} response directed toward SpCas9. However, when SpCas9-reactive T_{reg} cells were added to this assay, we detected a decrease in T_{eff}-mediated cytotoxicity in all donors, although the effect was small (Fig. 3h,i and Supplementary Fig. 10c–e). Of note, broadly activated T_{reg} cells were less potent in suppressing SpCas9-reactive $CD4^+$ T_{eff} proliferation and did not alter the killing capacity of SpCas9-reactive T_{eff} in eradicating transfected target cells (Supplementary Fig. 10c,d,f).

Our in vitro data indicate that endogenous SpCas9-reactive T_{reg} cells have the potential to mitigate the activation, expansion, and function of SpCas9-reactive T_{eff}, but future studies need to elucidate whether they harbor SpCas9-specific TCRs. Recent preclinical and first clinical data show that adoptively transferred T_{reg} cells can combat T cell priming but also overwhelming T_{eff} responses[28,29]. Hence, adoptive transfer of ex vivo enriched SpCas9-reactive T_{reg} cells or T_{reg} cells genetically modified to express SpCas9-specific TCRs may be a therapeutic option. We expect that most adults have protective antibodies directed against the integument proteins of pathogens. In this case, transfer of SpCas9-reactive T_{reg} cells should be a safe approach because T_{reg} cells are not known to block or inhibit the secretion of antibodies by plasma cells. Importantly, *S. pyogenes* is only a facultative intracellular pathogen. Hence, suppression of SpCas9-reactive $CD8^+$ T cells may not impact the overall antimicrobial immune response.

What might be the physiological significance of SpCas9-reactive T_{reg} cells? Bacterial colonization requires homeostasis between the host and the microbiota for optimal coexistence. This interplay is tightly mediated by microbe-specific T_{reg} cells. Prominently, patients suffering from immunodysregulation polyendocrinopathy enteropathy X-linked syndrome who lack functional T_{reg} cells fail to establish a healthy commensal flora, resulting in multiple immunopathologies[30]. Interestingly, *S. pyogenes* infection–associated diseases leading to systemic complications, such as rheumatic heart disease or poststreptococcal glomerulonephritis, occur predominantly in children and adolescencts[7]. The pathophysiology is believed to involve molecular mimicry that induces crossreactive antibodies by T helper cells[31]. However, T helper cell–mediated inflammation is controlled by T_{reg} cells. Therefore, future studies should test whether a misbalanced *S. pyogenes*–specific T_{reg}/T_{eff} response may be related to *S. pyogenes*–associated systemic disease.

In conclusion, our findings imply the need to test and potentially control the SpCas9-reactive T_{eff} response for successful CRISPR–Cas9 gene editing in vivo. Other commonly used SpCas9 orthologs, such as SaCas9 and Cpf1, pose similar risks through preexisting T cell sensitization. Our data are complemented by an article from Simhadri et al.[32] and a preprint article by Charlesworth et al.[8] (waiting to undergo peer review), which reported SpCas9- and SaCas9-specific antibodies in the serum of healthy humans and identified SaCas9-activated but not SpCas9-reactive T cells, due to low sensitivity for antigen-reactive T cells within their assays. The combined results suggest that it might be necessary to monitor the Cas-reactive adaptive immune responses before and during clinical trials employing Cas-derived therapeutic approaches to identify potentially high-risk patients. Therefore, misbalanced T_{reg}/T_{eff} ratios and strong $CD8^+$ T cell responses to Cas proteins in certain patients may pose limitations on Cas-associated gene therapy. Gene editing with only transient Cas exposure may reduce the risk for hazardous immunologic events. Of note, ex vivo modification using the CRISPR–Cas system might be less affected by immunogenicity if prolonged ex vivo culture is feasible because the gene-edited cells can be infused after complete degradation of the Cas protein. The unresponsiveness of autologous Cas-reactive T_{eff} cell lines to stimulation with CRISPR–Cas-edited cell samples could be a release criterion for cell/tissue products in CRISPR–Cas-related gene therapy (Fig. 3). For in vivo application of CRISPR–Cas, immunosuppressive treatment could be considered. Immunosuppressive drugs discussed for adeno-associated virus-related gene therapy in naive recipients, such as anti-CTLA4 antibodies and low-dose prednisone, are inadequate to control a preexisting T_{eff} cell response[33]. Further studies should elucidate whether the adoptive transfer of Cas-reactive T_{reg} cells can efficiently prevent hazardous inflammatory damage to CRISPR–Cas-edited tissues; this would circumvent the need for global immunosuppression.

URLs. UniProt, https://www.uniprot.org/; BLAST (Basic Local Alignment Search Tool), https://blast.ncbi.nlm.nih.gov/Blast.cgi.

Online content

Any methods, additional references, Nature Research reporting summaries, source data, statements of data availability and associated accession codes are available at https://doi.org/10.1038/s41591-018-0204-6.

Received: 11 March 2018; Accepted: 16 August 2018;
Published online: 29 October 2018

References

1. Jinek, M. et al. A programmable dual-RNA-guided DNA endonuclease in adaptive bacterial immunity. *Science* **337**, 816–821 (2012).
2. Cox, D. B. T., Platt, R. J. & Zhang, F. Therapeutic genome editing: prospects and challenges. *Nat. Med.* **21**, 121–131 (2015).
3. Chew, W. L. et al. A multifunctional AAV–CRISPR–Cas9 and its host response. *Nat. Methods* **13**, 868–874 (2016).
4. Chew, W. L. Immunity to CRISPR Cas9 and Cas12a therapeutics. *Wiley Interdiscip. Rev. Syst. Biol. Med.* **10**, e1408 (2018).
5. Lehrman, S. Virus treatment questioned after gene therapy death. *Nature* **401**, 517–518 (1999).
6. Nayak, S. & Herzog, R. W. Progress and prospects: immune responses to viral vectors. *Gene Ther.* **17**, 295–304 (2010).
7. Carapetis, J. R., Steer, A. C., Mulholland, E. K. & Weber, M. The global burden of group A streptococcal diseases. *Lancet. Infect. Dis.* **5**, 685–694 (2005).
8. Charlesworth, C. T. et al. Identification of pre-existing adaptive immunity to Cas9 proteins in humans. Preprint at https://www.biorxiv.org/content/early/2018/01/05/243345 (2018).
9. Kleinstiver, B. P. et al. High-fidelity CRISPR–Cas9 nucleases with no detectable genome-wide off-target effects. *Nature* **529**, 490–495 (2016).
10. Komor, A. C., Kim, Y. B., Packer, M. S., Zuris, J. A. & Liu, D. R. Programmable editing of a target base in genomic DNA without double-stranded DNA cleavage. *Nature* **533**, 420–424 (2016).
11. Vakulskas, C. A. et al. A high-fidelity Cas9 mutant delivered as a ribonucleoprotein complex enables efficient gene editing in human hematopoietic stem and progenitor cells. *Nat. Med* **24**, 1216–1224 (2018).
12. Shaikh, N., Leonard, E. & Martin, J. M. Prevalence of streptococcal pharyngitis and streptococcal carriage in children: a meta-analysis. *Pediatrics* **126**, e557–e564 (2010).
13. Frentsch, M. et al. Direct access to $CD4^+$ T cells specific for defined antigens according to CD154 expression. *Nat. Med.* **11**, 1118–1124 (2005).
14. Wolfl, M. et al. Activation-induced expression of CD137 permits detection, isolation, and expansion of the full repertoire of $CD8^+$ T cells responding to antigen without requiring knowledge of epitope specificities. *Blood* **110**, 201–210 (2007).
15. Schmueck-Henneresse, M. et al. Peripheral blood-derived virus-specific memory stem T cells mature to functional effector memory subsets with self-renewal potency. *J. Immunol.* **194**, 5559–5567 (2015).
16. Lathrop, S. K. et al. Peripheral education of the immune system by colonic commensal microbiota. *Nature* **478**, 250–254 (2011).
17. Bacher, P. et al. Regulatory T Cell specificity directs tolerance versus allergy against aeroantigens in humans. *Cell* **167**, 1067–1078.e16 (2016).
18. Sakaguchi, S., Sakaguchi, N., Asano, M., Itoh, M. & Toda, M. Immunologic self-tolerance maintained by activated T cells expressing IL-2 receptor alpha-chains (CD25). Breakdown of a single mechanism of self-tolerance causes various autoimmune diseases. *J. Immunol.* **155**, 1151–1164 (1995).

19. Hori, S., Nomura, T. & Sakaguchi, S. Control of regulatory T Cell development by the transcription factor *Foxp3*. *Science* **299**, 1057–1061 (2003).
20. Wing, K. et al. CTLA-4 contrÿol over Foxp3^{+} regulatory T cell function. *Science* **322**, 271–275 (2008).
21. Schoenbrunn, A. et al. A converse 4-1BB and CD40 ligand expression pattern delineates activated regulatory T cells (T_{reg}) and conventional T cells enabling direct isolation of alloantigen-reactive natural Foxp3^{+} T_{reg}. *J. Immunol.* **189**, 5985–5994 (2012).
22. Polansky, J. K. et al. DNA methylation controls *Foxp3* gene expression. *Eur. J. Immunol.* **38**, 1654–1663 (2008).
23. Bacher, P. et al. Antigen-specific expansion of human regulatory T cells as a major tolerance mechanism against mucosal fungi. *Mucosal Immunol.* **7**, 916–928 (2014).
24. Shmakov, S. et al. Diversity and evolution of class 2 CRISPR–Cas systems. *Nat. Rev. Microbiol.* **15**, 169–182 (2017).
25. Harrison, O. J. & Powrie, F. M. Regulatory T cells and immune tolerance in the intestine. *Cold Spring Harb. Perspect. Biol.* **5**, a018341 (2013).
26. Wakelin, S. J. et al. "Dirty little secrets": endotoxin contamination of recombinant proteins. *Immunol. Lett.* **106**, 1–7 (2006).
27. Hamano, R., Huang, J., Yoshimura, T., Oppenheim, J. J. & Chen, X. TNF optimally activatives regulatory T cells by inducing TNF receptor superfamily members TNFR2, 4-1BB and OX40. *Eur. J. Immunol.* **41**, 2010–2020 (2011).
28. Lei, H., Schmidt-Bleek, K., Dienelt, A., Reinke, P. & Volk, H.-D. Regulatory T cell-mediated anti-inflammatory effects promote successful tissue repair in both indirect and direct manners. *Front. Pharmacol.* **6**, 184 (2015).
29. Chandran, S. et al. Polyclonal regulatory T Cell therapy for control of inflammation in kidney transplants. *Am. J. Transplant.* **17**, 2945–2954 (2017).
30. Bennett, C. L. et al. The immune dysregulation, polyendocrinopathy, enteropathy, X-linked syndrome (IPEX) is caused by mutations of *FOXP3*. *Nat. Genet.* **27**, 20–21 (2001).
31. Guilherme, L., Kalil, J. & Cunningham, M. Molecular mimicry in the autoimmune pathogenesis of rheumatic heart disease. *Autoimmunity* **39**, 31–39 (2006).
32. Simhadri, V. L. et al. Prevalence of pre-existing antibodies to CRISPR-associated nuclease Cas9 in the USA population. *Mol. Ther. Methods Clin. Dev* **10**, 105–112 (2018).
33. Arruda, V. R., Favaro, P. & Finn, J. D. Strategies to modulate immune responses: a new frontier for gene therapy. *Mol. Ther.* **17**, 1492–1503 (2009).

Acknowledgements

The study was generously supported in parts by the Deutsche Forschungsgemeinschaft (German Research Foundation, SFB-TR36-project A3 grant to H.-D.V., P.R., M.S.H.), the German Federal Ministry of Education and Research (BCRT grant, all authors), a kick-box grant for young scientists by the Einstein Center for Regenerative Therapies (D.L.W.), and the Berlin Institute of Health medical doctoral research stipend (D.L.W.). The funders had no role in the study design, data collection and analysis, decision to publish, or preparation of the manuscript. We would like to acknowledge the assistance of the BCRT Flow & Mass Cytometry Lab, D. Kunkel and J. Hartwig; G. Grütz and the team of the Core Unit Biomarker—Immunological Study Lab, BCRT, Charité—Universitätsmedizin Berlin; M. Streitz for flow cytometry assistance and CMV lysates; K. Vogt for technical assistance with the TSDR analyses; A. Jurisch, K. Grzeschik, and R. Noster for technical assistance; and A. Floriane Hennig and U. Kornak (Institute for Medical Genetics and Human Genetics, Charité – Universitätsmedizin Berlin) for the PX458_T2mali DNA plasmid. We thank the groups of M. Seifert and A. Thiel (both BCRT, Charité—Universitätsmedizin Berlin) for supplying the reagents, and T. Roch and M. Frentsch for critical discussions.

Author contributions

D.L.W. led the project, designed the research, performed the experiments, analyzed and interpreted the data, and wrote the manuscript. L. Amini and D.J.W. established the methods, performed the experiments, analyzed the data, and revised the manuscript. L.-M.B. performed the experiments. L. Akyüz designed the experimental approaches, and performed the Meso Scale Diagnostics and Ella systems measurements. P.R. wrote the manuscript and supplied the reagents. H.-D.V. designed the research, interpreted the data, and wrote the manuscript. M.S.-H. led the project, designed the research, analyzed and interpreted the data, and wrote the manuscript.

Competing interests

D.L.W., L. Amini, D.J.W., M.S.-H., P.R., and H.-D.V. have a patent pending on CRISPR Associated Protein Reactive T Cell Immunity (European patent application EP18163491.6, 2018). L.-M.B. and L. Akyüz have no financial competing interests.

Additional information

Supplementary information is available for this paper at https://doi.org/10.1038/s41591-018-0204-6.

Reprints and permissions information is available at www.nature.com/reprints.

Correspondence and requests for materials should be addressed to M.S.-H.

Publisher's note: Springer Nature remains neutral with regard to jurisdictional claims in published maps and institutional affiliations.

Methods

Cell preparation. We collected blood samples from healthy volunteers after obtaining informed consent. We separated PBMCs from the heparinized whole blood of healthy donors (median age: 34; range: 18–60, 24 women/24 men) by lymphoprep density gradient centrifugation with a Biocoll separating solution (Biochrom GmbH, Berlin). PBMCs were cultured in complete medium, comprising very-low-endotoxin-Roswell Park Memorial Institute (RPMI) 1640 medium supplemented with stable glutamine, 100 U ml^{-1} penicillin, 0.1 mg ml^{-1} streptomycin (all from Biochrom) and 10% heat-inactivated fetal bovine serum (PAA Laboratories).

This study was approved by the Charité University Medical School Ethical Committee (institutional review board). Informed consent was documented.

Flow cytometric analysis. We pulsed freshly isolated PBMCs with antigen at a 10-fold concentration for 10 min and subsequently stimulated them in polystyrene round-bottom tubes (Falcon; Corning) at 37 °C and 5% CO_2 in humidified incubators for 16 h. Antigens and final concentrations were: 5 µg ml^{-1} SpCas9 (PNA Bio); 1 µg ml^{-1} SEB (Sigma); CMV lysate (generously provided by Mathias Streitz) and CMV pp65 overlapping peptide pool at 1 µg ml^{-1} (15mers with an 11 amino acid (aa) overlap; JPT Peptide Technologies); 3 µg ml^{-1} recombinant SaCas9 (Applied Biological Materials); and 5 µg ml^{-1} recombinant Cpf1 nuclease (Cpf1, Cas12a) (Integrated DNA Technologies).

Where indicated, PBMCs were depleted for $CD4^+$ or $CD25^+$ cells using MicroBeads (Miltenyi Biotech), following the manufacturer's instructions. To exclude endotoxin contamination, 10 µg ml^{-1} BPI (Sigma-Aldrich) was applied during stimulation. For functional and phenotypic characterization, 5×10^6 PBMCs per 1 ml complete medium were stimulated. Where indicated, 15 µg ml^{-1} of MHC class II–blocking antibody (LEAF purified anti–human HLA-DR antibody; BioLegend) was applied during stimulation.

In particular experiments, polyclonal T_{reg} cells were enriched in bulk by FACS, as described in the SpCas9-reactive T cell isolation section of the Methods, according to the cell surface expression of $CD4^+CD25^+$ $CD127^-$, rested overnight at 37 °C and 5% CO_2 in humidified incubators and subsequently stimulated with 5 µg ml^{-1} SpCas9-pulsed monocytes (sorted according to the side scatter/forward scatter (FSC) profile) and B cells (sorted $CD3^-$ fraction). Intracellular, T_{reg}-specific FOXP3 transcription factor staining was performed post-sorting. Post-sorting analysis of purified T_{reg} cells revealed purities >95%.

For analysis of antigen-induced intracellular CD154 and CD137 expression and IFN-γ, TNF-α, and IL-2 production, we added 10 µg ml^{-1} of brefeldin A (Sigma-Aldrich). To allow for sufficient SpCas9 antigenic APC processing and presentation, brefeldin A was only added for the last 10 h of stimulation. After cell collection, extracellular T cell memory phenotype staining was performed using fluorescently conjugated monoclonal antibodies for CCR7 (PE, clone G043H7), CD45RA (PE/Dazzle 594, clone HI100), and CD45RO (Brilliant Violet (BV) 785, clone UCHL1) at 4 °C for 30 min. In some of the experiments, CD25 (APC, clone 2A3; BD Biosciences), CD127 (APC Alexa Fluor 700, clone R34.34; Beckman Coulter), and CD152 (CTLA-4) (PE-Cy5, clone BNI3; BD Biosciences) antibodies were used to define T_{reg}-specific surface molecule expression. To exclude dead cells, LIVE/DEAD Fixable Blue Dead Cell Stain dye (Thermo Fisher Scientific) was added. Subsequently, cells were fixed and permeabilized with an eBioscience FoxP3/Transcription Factor Staining Buffer Set (Thermo Fisher Scientific), according to the manufacturer's instructions. After washing, we stained the fixed cells at 4 °C with the following fluorochrome-conjugated monoclonal antibodies for 30 min: FOXP3 (Alexa Fluor 488, clone: 259D); CD3 (BV650, clone OKT3); CD4 (PerCP-Cy5.5, clone SK3); CD8 (BV570, clone RPA-T8); CD137 (PE/Cy7, clone 4B4-4); CD154 (BV711, clone 24–31); IFN-γ (BV605, clone 4S.B3); TNF-α (Alexa Fluor 700, clone MAb11); and IL-2 (BV421, clone MQ1-17H12). In some of the experiments, a monoclonal antibody against CD107a (BV785 clone: H4A3) was added at the very start of the stimulation. In some of the experiments, antibodies for the intracellular fluorescence staining of T-bet (Alexa Fluor 647, clone 4B10) and FOXP3 were used to define T cell lineage, to determine the levels of transcription factor expression. All antibodies were purchased from BioLegend, unless otherwise indicated. Cells were analyzed on an LSR-II FORTESSA flow cytometer (BD Biosciences) and FlowJo software version 10 (Tree Star). For ex vivo analysis, at least 2×10^6 events were recorded. Lymphocytes were gated on the basis of the FSC versus side scatter profile and subsequently gated on FSC-Height versus FSC to exclude doublets. Unstimulated PBMCs were used as controls; the respective background responses were subtracted from antigen-reactive cytokine production (Fig. 1). Negative values were set to zero.

SpCas9-reactive T cell isolation. *Isolation.* We separated PBMCs from 80 ml heparinized whole blood. We washed PBMCs twice with PBS and resuspended the cell pellets at one-tenth of the finale culture volume supplemented with 50 µg ml^{-1} SpCas9 whole protein (PNA Bio). After 15 min, the volume was adjusted to 1×10^7 cells ml^{-1}. We incubated them in the presence of 5 µg ml^{-1} SpCas9 whole protein and 1 µg ml^{-1} CD40-specific antibody (HB 14; Miltenyi Biotech) at cell concentrations of 1×10^7 PBMCs per 1 ml very-low-endotoxin-RPMI 1640 medium with stable glutamine supplemented with 100 U ml^{-1} penicillin, 0.1 mg ml^{-1} streptomycin and 5% heat-inactivated human AB serum (PAA Laboratories) in polystyrene flat-bottom 24-well plates (Falcon; Corning) at 37 °C and 5% CO_2 in humidified incubators for 16 h. After stimulation, cells were washed with PBS (0.5% BSA) and stained with fluorochrome-conjugated antibodies specific for: CD3 (BV650, clone OKT3); CD4 (PerCP-Cy5.5, clone SK3); CD25 (APC, clone 2A3); CD127 (APC Alexa Fluor 700, clone R34.34; Beckman Coulter); CD137 (PE/Cy7, clone 4B4-4); and CD154 (BV711, clone 24-31) for 10 min. SpCas9-reactive T_{reg} (Supplementary Fig. 5a: $CD3^+CD4^+CD137^+CD154^-CD25^{hi}CD127^-$) and SpCas9-reactive T_{eff} (Supplementary Fig. 5a: $CD3^+CD137^+CD154^+CD25^{lo}$) were enriched by FACS on a BD FACSAria II SORP (BD Biosciences), performed by the Flow Cytometry and Mass Cytometry Lab of the Berlin-Brandenburg Center for Regenerative Therapies (BCRT, D. Kunkel and J. Hartwig). In addition, polyclonal T_{reg} (Supplementary Fig. 5: $CD3^+CD4^+CD137^-CD154^-CD25^{hi}CD127^-$) and polyclonal T_{eff} (Supplementary Fig. 5: $CD3^+CD137^-CD154^-CD25^{lo}$) cells were enriched for nonspecific expansion. Intracellular T_{reg}-specific FOXP3 transcription factor staining was performed post-sorting. Post-sorting analysis of purified subsets revealed purities >90%.

TNF-α release assay for testing endotoxin contamination. To test for the potential endotoxin contamination of the recombinant Cas proteins, detection of human TNF-α in supernatants of whole blood was performed with the Ella system assay (ProteinSimple), according to the manufacturer's instructions. TNF-α release was assessed in the whole blood assay by the given reagent alone and in presence of 10 µg ml^{-1} BPI. Heparinized whole blood from healthy volunteers was diluted 1:10 with RPMI medium and stimulated with either 500 ng ml^{-1} lipopolysaccharide, 25 ng ml^{-1} phorbol myristate acetate/2 µg ml^{-1} ionomycin, 1 µg ml^{-1} SEB, CMV pp65 overlapping peptide pools at 1 µg ml^{-1} or 5 µg ml^{-1} SpCas9/SaCas9/Cpf1 for 24 h at 37 °C. After centrifugation for 15 min at 1,000*g* at room temperature, the supernatants were collected. Measurements were performed in the Immunological Study Lab of the BCRT. For each sample, the respective optical density values of TNF-α concentration calculated on the basis of a calibration curve were obtained by subtracting the blank provided by the vendor. The mean concentrations and standard deviations of the samples were calculated.

Proliferation assay. PBMCs were labeled with 10 µM carboxyfluorescein succinimidyl ester (CFSE; Thermo Fisher Scientific), activated with SpCas9 whole protein, and cultured in complete medium for 5 d in the presence or absence of MHC class II -blocking antibody (MHC class II :HLA-DR). The frequencies of T cell proliferation (CFSE dilution) were assessed by flow cytometry following 5 d of culture.

Proliferation suppression assay. SpCas9-reactive T_{reg}, SpCas9-reactive T_{eff}, and polyclonal T_{eff} cells were enriched as described in the SpCas9-reactive T cell isolation section. T_{eff} were labeled with 10 µM CFSE; Molecular Probes). CFSE-labeled SpCas9-reactive T_{eff} or polyclonal T_{eff} cells were cultured in complete medium alone or with autologous SpCas9-reactive T_{reg} at T_{eff}/T_{reg} ratios of 1:1 and 5:1. Polyclonal T_{eff} were stimulated with anti-CD3/CD28-coated microbeads (T_{reg} suppression inspector; Miltenyi Biotech) at a cell per bead ratio of 1:1 adjusted to the total cell number per well and incubated at 37 °C for 96 h. SpCas9-reactive T_{eff} were activated before sorting with no further stimulation and incubated at 37 °C for 96 h. Thereafter, cells were stained with CD3 (BV650, clone OKT3) and CD4 (PerCP-Cy5.5, clone SK3), all sourced from BioLegend. Dead cells were excluded using the LIVE/DEAD Fixable Aqua Dead Cell Stain Kit (Invitrogen). Proliferation was assessed by CFSE dilution; the percentage suppression of proliferation was calculated by relating the percentage of proliferating T_{eff} cells in the presence and absence of T_{reg}, respectively.

Assessment of cytokines in supernatants (the Meso Scale Diagnostics method). Culture supernatants from the 96-h proliferation suppression assay were collected, and cytokines were assessed using the human Proinflammatory Panel 1 kit (for IFN-γ, IL-10, IL-2, and TNF-α; Meso Scale Diagnostics), following the manufacturer's instructions. Measurements were performed at the Immunological Study Lab of the BCRT on a Mesoscale Discovery platform. For each sample, the respective optical density values of the analyte concentration, calculated on the basis of a calibration curve, were obtained by subtracting the blank. The mean concentrations and standard deviations of the samples were calculated. The measurements of the Meso Scale Diagnostics assay were performed and evaluated in accordance with the International Conference on Harmonisation Good Clinical Practice Guideline under 'Validation of analytical procedures'.

TCR next-generation sequencing. The genomic DNA of freshly sorted SpCas9-reactive and polyclonal $CD4^+$ T_{reg} and T_{eff} cells was isolated using the Quick-DNA Miniprep Plus Kit (Zymo Research) according to the manufacturer's instructions, with a final elution volume of 40 µl DNase-free elution buffer. Complementary determining region 3 sequencing was performed using the immunoSEQ platform at Adaptive Biotechnologies as previously described by Robins et al.[34]. and Sherwood et al.[35]. Data were evaluated with the immunoSEQ Analyzer 3.0 developed by Adaptive Biotechnologies and previously described by Monod et al.[36].

Serological testing for previous exposure to *S. pyogenes*. Peripheral blood from healthy donors was sampled into a container for serum preparation (VACUETTE;

Greiner Bio-One). The blood was centrifuged at 1,000*g* for 10 min; the serum supernatant was carefully collected and transferred into a sterile serum container for analysis (SARSTEDT). Subsequently, the serum samples were sent to a diagnostic laboratory (Labor Berlin GmbH) for a standardized assessment of serum antibody concentrations directed to known *S. pyogenes* antigens—exotoxin streptolysin O and streptococcal DNase B. Serum titers above 200 IE ml^{-1} are highly suggestive of exposure within recent weeks or months. Lower serum levels indicate previous exposure[37,38].

Allocation and culture of LCLs. SpCas9-reactive T lymphocytes were analyzed for effector functions by their ability to recognize SpCas9-transfected target cells, that is, autologous LCLs transformed with B95-8 Epstein–Barr virus as described previously[39,40]. Autologous primary Epstein–Barr virus-transformed LCLs were cultured in very-low-endotoxin RPMI 1640 medium supplemented with stable glutamine, 100 U ml^{-1} penicillin, 0.1 mg ml^{-1} streptomycin (all from Biochrom) and 10% heat-inactivated fetal bovine serum (PAA Laboratories).

Transfection of primary LCLs. Most in vivo gene therapeutic approaches using CRISPR–Cas9 aim to endogenously express SpCas9 and the respective single guide RNA within the target cell through viral or nonviral vectors. To determine the immunogenicity of endogenously expressed SpCas9, we transfected autologous LCLs with a DNA plasmid vector containing an expression cassette for SpCas9; 24–36 h before transfection, LCLs were seeded at a concentration between 2.5 and 5.0×10^5 cells per ml of antibiotic-free cell culture medium. For transfection, LCLs were collected and washed twice with PBS. Cell pellets were resuspended at 1×10^7 cells per ml Buffer R and supplemented with either pMAX-GFP (Lonza) with a final concentration of 25 µg ml^{-1} as control or a SpCas9-expressing plasmid (PX458) with a final concentration of 100 µg ml^{-1}. pSpCas9(BB)-2A-GFP (PX458) was kindly provided by F. Zhang (Addgene)[41]. The PX458 plasmid contains a fusion protein of the *S. pyogenes* Cas9 nuclease and the GFP connected by the self-cleaving peptide P2A. After protein translation, P2A leads to the separation of single SpCas9 and a GFP protein, respectively. We used a modified PX458 plasmid containing a single guide RNA targeting the hAAVS1 locus[42], generously provided by A.-F. Hennig and U. Kornak. Transfection of LCLs was performed using 10 µl tips of the Neon Transfection System (Thermo Fisher Scientific) by electroporation with 3 pulses at 1,600 V for 10 ms. After electroporation, LCLs were directly transferred to prewarmed antibiotic-free medium and rested for 24 h before performing the cytotoxicity assays.

Assessment of cytotoxic activity: VITAL assay. A modified VITAL assay was used for cytotoxicity testing as described previously[15,41]. Briefly, transfected LCLs expressing SpCas9 and GFP (LCLs-SpCas9$^+$GFP$^+$) served as SpCas9-positive target cells for T cells and LCLs expressing GFP alone (LCLs-GFP$^+$) served as SpCas9-negative target cells for T cells to exclude unspecific killing due to DNA plasmid electroporation and GFP expression. As internal controls, unmodified LCLs were labeled with 5 µM *N*,*N*-dimethyldodecylamine *N*-oxide (Invitrogen).

T cell enrichment. We cultured isolated SpCas9-reactive T_{eff} cells in a U-bottom 96-well plate (Falcon; Corning) with RPMI medium containing 5% human AB serum including recombinant human IL-7 and IL-15 each at 10 ng ml^{-1} (CellGenix) at 37 °C and 5% CO_2 in humidified incubators for 3 d. We cultured isolated SpCas9-reactive T_{reg} cells in a U-bottom 96-well plate with RPMI medium containing 5% human AB serum including 500 IU ml^{-1} recombinant human IL-2 (Proleukin; Novartis) at 37 °C and 5% CO_2 in humidified incubators for 3 d.

Setting up the cytotoxicity assay. Target and nontarget LCLs were cocultured for 16 h with SpCas9-reactive T cell/target cell ratios of 10:1, 1:1, and 1:10 (for electroporation; see the Transfection of primary LCLs section of the Methods). Samples without T cells, containing only targets and nontargets (LCL-SpCas9$^+$GFP$^+$/LCL-GFP$^+$ and *N*,*N*-dimethyldodecylamine *N*-oxide-labeled unmodified LCLs), served as reference controls. After coculture, the cells were analyzed using the LSR-II Fortessa flow cytometer (BD Biosciences). Dead cells were excluded using the LIVE/DEAD Fixable Blue Dead Cell Stain dye (Thermo Fisher Scientific). The mean percentage survival of LCL-SpCas9$^+$GFP$^+$ target cells or LCL-GFP$^+$ cells was calculated relative to the *N*,*N*-dimethyldodecylamine *N*-oxide-labeled unmodified LCL controls. Subsequently, the percentage of specific target cell lysis was calculated, comparing the mean percent survival of targets in cultures containing defined numbers of T_{eff} cells and the conditions without T cells.

TSDR methylation analysis. DNA methylation analysis of the TSDR was performed as previously described[22]. Briefly, bisulfite-modified (EpiTect Bilsulfite Kit; QIAGEN) genomic DNA isolated using the Quick-DNA Miniprep Plus Kit (Zymo Research) was used in a real-time PCR for FOXP3 TSDR quantification. A minimum of 40 ng genomic DNA or a respective amount of plasmid standard was used in addition to 10 µl FastStart Universal Probe Master (Roche Life Science), 50 ng $µl^{-1}$ Lambda DNA (New England Biolabs), 5 pmol $µl^{-1}$ methylation or nonmethylation-specific probe, 30 pmol $µl^{-1}$ methylation or nonmethylation-specific primers (both from Epiontis) in 20 µl of total reaction volume. The samples were analyzed in triplicates on an ABI 7500 cycler (Thermo Fisher Scientific).

Comparison of Cas protein sequences. The protein sequence of SpCas9 and its homologs was derived from the UniProt database (see URLs). Subsequently, the SpCas9 sequence (UniProt accession number Q99ZW2) was aligned to either the sequence of SaCas9 (UniProt accession number J7RUA5) and Cpf1 (UniProt accession number U2UMQ6) using the blastp suite algorithm (protein-protein BLAST, see URLs)[43].

Statistical analysis. GraphPad Prism 7 (GraphPad Software) was used to generate graphs and carry out the statistical analysis of data. To test for a normal Gaussian distribution, the D'Agostino and Pearson normality test was performed. If sample size was insufficient for the D'Agostino and Pearson normality test, a Kolmogorov–Smirnov test was employed. When comparing two datasets, if data were normally distributed, a Student's paired *t*-test was employed to analyze the data. If data were not normally distributed, a Wilcoxon signed-rank test was applied. All tests were two-tailed. When more than two paired datasets were compared, a one-way ANOVA was employed for normally distributed samples and a Friedman test was used for not normally distributed samples. For comparison of more than two unpaired non-normally distributed datasets, we applied the Kruskal–Wallis test. To exactly identify significant differences in non-normally distributed datasets, Dunn's multiple comparison test was used as a post hoc test; the post hoc test employed for normally distributed samples was Tukey's multiple comparison test. Correlation analysis was assessed with Pearson correlation coefficients for normally distributed data or nonparametric Spearman's rank correlation for non-normally distributed data. The regression line was inserted based on linear regression analysis. *P* values ≤ 0.05 were considered statistically significant and significance was denoted as follows: $^*P \leq 0.05$; $^{**}P \leq 0.01$; $^{***}P \leq 0.001$; $^{****}P \leq 0.0001$.

Accession codes. The protein sequences of SpCas9 and its homologs SaCas9 and Cpf1 were derived from the UniProt database (see earlier in the text).

Reporting summary. Further information on research design is available in the Nature Research Reporting Summary linked to this article.

Data availability

The underlying data are available from the corresponding author upon reasonable request. TRB sequencing data have been deposited in the immuneACCESS database at https://doi.org/10.21417/B7ZP86 (http://clients.adaptivebiotech.com/pub/wagner-2018-naturemedicine).

References

34. Robins, H. S. et al. Comprehensive assessment of T-cell receptor beta-chain diversity in alphabeta T cells. *Blood* **114**, 4099–4107 (2009).
35. Sherwood, A. M. et al. Deep sequencing of the human TCRγ and TCRβ repertoires suggests that TCRβ rearranges after αβ and γδ T cell commitment. *Sci. Transl. Med.* **3**, 90ra61 (2011).
36. Yousfi Monod, M. Y., Giudicelli, V., Chaume, D. & Lefranc, M.-P. IMGT/JunctionAnalysis: the first tool for the analysis of the immunoglobulin and T cell receptor complex V-J and V-D-J JUNCTIONs. *Bioinformatics* **20**, i379–i385 (2004).
37. Johnson, D. R., Kurlan, R., Leckman, J. & Kaplan, E. L. The human immune response to streptococcal extracellular antigens: clinical, diagnostic, and potential pathogenetic implications. *Clin. Infect. Dis.* **50**, 481–490 (2010).
38. Sen, E. S. & Ramanan, A. V. How to use antistreptolysin O titre. *Arch. Dis. Child. Educ. Pract. Ed.* **99**, 231–238 (2014).
39. Heslop, H. E. et al. Long-term restoration of immunity against Epstein–Barr virus infection by adoptive transfer of gene-modified virus-specific T lymphocytes. *Nat. Med.* **2**, 551–555 (1996).
40. Moosmann, A. et al. B cells immortalized by a mini-Epstein–Barr virus encoding a foreign antigen efficiently reactivate specific cytotoxic T cells. *Blood* **100**, 1755–1764 (2002).
41. Ran, F. A. et al. Genome engineering using the CRISPR–Cas9 system. *Nat. Protoc.* **8**, 2281–2308 (2013).
42. Mali, P. et al. RNA-guided human genome engineering via Cas9. *Science* **339**, 823–826 (2013).
43. Johnson, M. et al. NCBI BLAST: a better web interface. *Nucleic Acids Res.* **36**, W5–W9 (2008).
44. Hammoud, B. et al. HCMV-specific T-cell therapy: do not forget supply of help. *J. Immunother.* **36**, 93–101 (2013).

nature research

Corresponding author(s): M. Schmueck-Henneresse

Reporting Summary

Nature Research wishes to improve the reproducibility of the work that we publish. This form provides structure for consistency and transparency in reporting. For further information on Nature Research policies, see Authors & Referees and the Editorial Policy Checklist.

Statistical parameters

When statistical analyses are reported, confirm that the following items are present in the relevant location (e.g. figure legend, table legend, main text, or Methods section).

n/a	Confirmed	
☐	☒	The exact sample size (*n*) for each experimental group/condition, given as a discrete number and unit of measurement
☐	☒	An indication of whether measurements were taken from distinct samples or whether the same sample was measured repeatedly
☐	☒	The statistical test(s) used AND whether they are one- or two-sided *Only common tests should be described solely by name; describe more complex techniques in the Methods section.*
☐	☒	A description of all covariates tested
☐	☒	A description of any assumptions or corrections, such as tests of normality and adjustment for multiple comparisons
☐	☒	A full description of the statistics including central tendency (e.g. means) or other basic estimates (e.g. regression coefficient) AND variation (e.g. standard deviation) or associated estimates of uncertainty (e.g. confidence intervals)
☒	☐	For null hypothesis testing, the test statistic (e.g. *F*, *t*, *r*) with confidence intervals, effect sizes, degrees of freedom and *P* value noted *Give P values as exact values whenever suitable.*
☒	☐	For Bayesian analysis, information on the choice of priors and Markov chain Monte Carlo settings
☒	☐	For hierarchical and complex designs, identification of the appropriate level for tests and full reporting of outcomes
☐	☒	Estimates of effect sizes (e.g. Cohen's *d*, Pearson's *r*), indicating how they were calculated
☐	☒	Clearly defined error bars *State explicitly what error bars represent (e.g. SD, SE, CI)*

Our web collection on statistics for biologists may be useful.

Software and code

Policy information about availability of computer code

Data collection	The protein sequence of SpCas9 and its homologues was derived from the Uniprot database. Cells were analysed on a LSR-II Fortessa flow cytometer (BD Biosciences; BD FACSDIVA TM Software v8.0.2) and FlowJo Version 10 software (Tree Star).
Data analysis	Protein-protein alignement done with BLASTp suite 2.8.0 publicly available on NCBI. TCR sequencing data were evaluated using the immunoSEQ ANALYZER platform 3.0 developed by Adaptive Biotechnologies. Graph Pad Prism version 7 was used for generation of graphs and statistical analysis. FlowJo Version 10 software (Tree Star) for flow cytometry analyses.

For manuscripts utilizing custom algorithms or software that are central to the research but not yet described in published literature, software must be made available to editors/reviewers upon request. We strongly encourage code deposition in a community repository (e.g. GitHub). See the Nature Research guidelines for submitting code & software for further information.

Data

Policy information about availability of data

All manuscripts must include a data availability statement. This statement should provide the following information, where applicable:

- Accession codes, unique identifiers, or web links for publicly available datasets
- A list of figures that have associated raw data
- A description of any restrictions on data availability

The SpCas9 sequence (Uniprot accession: Q99ZW2) was aligned to either the sequence of (Uniprot accession: J7RUA5) and Cpf1 (Uniprot accession: U2UMQ6) using the blastp suite algorithm (protein-protein BLAST, NCBI, National Library of Medicine, USA). The underlying data are available from the corresponding author on reasonable request. TCRB sequencing data have been deposited in the ImmuneACCESS database under the accession code DOI:XXXXXX (http://clients.adaptivebiotech.com/pub/XXXXXXX). (in progress)

Field-specific reporting

Please select the best fit for your research. If you are not sure, read the appropriate sections before making your selection.

☒ Life sciences ☐ Behavioural & social sciences ☐ Ecological, evolutionary & environmental sciences

For a reference copy of the document with all sections, see nature.com/authors/policies/ReportingSummary-flat.pdf

Life sciences study design

All studies must disclose on these points even when the disclosure is negative.

Sample size	The number of stimulations for each experiment were determined based on past experience with antigenic stimulations for infection with high prevalence like CMV. No power analysis were performed prior to experiments to determine sample size. Due to high prevalence of S. pyogenes as verified by serological analyses we initially analyzed 24 donors and verfied data by with a validation cohort in another 24 donors upon request of reviewers.
Data exclusions	No data was excluded. Healthy human donors aged between 18-60 years were included in the study without any additional exclusion criteria.
Replication	All replication was successful.
Randomization	Healthy human donors were randomly selected for blood donation without a plan for randomization.
Blinding	These studies were not blinded. Blinding was not performed for age and gender matching.

Reporting for specific materials, systems and methods

Materials & experimental systems

n/a	Involved in the study
☒	☐ Unique biological materials
☐	☒ Antibodies
☐	☒ Eukaryotic cell lines
☒	☐ Palaeontology
☒	☐ Animals and other organisms
☐	☒ Human research participants

Methods

n/a	Involved in the study
☒	☐ ChIP-seq
☐	☒ Flow cytometry
☒	☐ MRI-based neuroimaging

Antibodies

Antibodies used	All antibodies were purchased from Biolegend, unless indicated otherwise: CCR7 (PE, clone: G043H7; dilution 1:50; CN: 353204), CD45RA (PE-Dazzle 594, clone: HI100; dilution 1:100; CN: 304146), CD45RO (BV785, clone: UCHL1; dilution 1:100; CN: 304234), CD25 (BD, APC, clone: 2A3; dilution 1:20; CN: 340907), CD127 (Beckman Coulter, APC-Alexa Fluor 700, clone: R34.34; dilution 1:10; CN: A71116), CD152 (CTLA-4) (BD, PE-Cy5, clone: BNI3; dilution 1:10; CN: 555854), LIVE/DEAD Fixable Blue Dead Cell Stain dye (Invitrogen; dilution 1:150; CN: L34962), FoxP3 (Alexa Fluor 488, clone: 259D; dilution 1:10; CN: 320212), CD3 (BV650, clone: OKT3; dilution 1:50; CN: 317324), CD4 (PerCp-Cy5.5, clone: SK3; dilution 1:100; CN: 344608) CD8 (BV570, clone: RPA-T8; dilution 1:100; CN: 301038), CD137 (PE-Cy7,

clone: 4B4-4; dilution 1:100; CN: 309818), CD154 (BV711, clone 24-31; dilution 1:100; CN: 310838), IFN-g (BV605, clone 4S.B3; dilution 1:20; CN: 502536), TNF- (Alexa Fluor 700, clone: MAb11; dilution 1:50; CN: 502928), IL-2 (BV421, clone MQ1-17H12; dilution 1:100; CN: 500328), CD107a (BV785 clone: H4A3; dilution 1:100; CN: 328644), Tbet (Alexa Fluor 647, clone: 4B10; dilution 1:100; CN: 644804)

Validation

Previously authenticated antibodies were purchased from BD, Biolegend, and eBioscience. Citation of their use is below
J Immunol June 1, 2015, 194 (11) 5559-5567
J Immunol May 15, 2012, 188 (10) 5189-5198

Eukaryotic cell lines

Policy information about cell lines

Cell line source(s)	Autologous lymphoblastoid B cell lines (LCLs) transformed with B95-8 EBV.
Authentication	Lymphoblastoid B cell lines were authenticated in their ability to stimulate autologous T cells.
Mycoplasma contamination	Cell lines are tested for mycoplasma contamination every 12 months.
Commonly misidentified lines (See ICLAC register)	Commonly misidentified cell lines were not used.

Human research participants

Policy information about studies involving human research participants

Population characteristics	Whole blood from healthy donors was used (median age: 34, range: 18-60, 24 female/ 24 male)
Recruitment	Recruitment was performed unbiased with random selection of healthy volunteers.

Flow Cytometry

Plots

Confirm that:

☐ The axis labels state the marker and fluorochrome used (e.g. CD4-FITC).

☒ The axis scales are clearly visible. Include numbers along axes only for bottom left plot of group (a 'group' is an analysis of identical markers).

☒ All plots are contour plots with outliers or pseudocolor plots.

☒ A numerical value for number of cells or percentage (with statistics) is provided.

Methodology

Sample preparation	We separated PBMCs from heparinized whole blood from healthy donors by lymphoprep density gradient centrifugation with a Biocoll-separating solution.
Instrument	LSR-II Fortessa System (BD Biosciences)
Software	FlowJo Version 10 software (Tree Star)
Cell population abundance	Intracellular TREG-specific FoxP3 transcription factor staining was performed post sorting. Post sorting analysis of purified subsets revealed purities over 90 %.
Gating strategy	For ex vivo analysis, at least 2x10e6 events were recorded. Lymphocytes were gated based on the FSC versus SSC profile and subsequently gated on FSC (height) versus FSC to exclude doublets. Unstimulated PBMCs were used as controls and respective background responses were subtracted from antigen-specific cytokine production. Negative values were set to zero.

☒ Tick this box to confirm that a figure exemplifying the gating strategy is provided in the Supplementary Information.